Fatigue & Fracture of Engineering Materials & Structures 1998; **21**: 1307–1316

FATIGUE CRACKING POSSIBILITY ALONG GRAIN BOUNDARIES AND PERSISTENT SLIP BANDS IN COPPER BICRYSTALS

Z. F. ZHANG, Z. G. WANG and S. X. LI

State Key Laboratory for Fatigue and Fracture of Materials, Institute of Metal Research, Chinese Academy of Sciences, Shenyang, 110015, P. R. China

Received in final form August 1997

Abstract—In this paper, the fatigue cracking possibility in different kinds of copper bicrystals with large-angle grain boundaries (GBs) and copper multicrystals containing some low-angle GBs are compared. The results showed that the fatigue cracks, in the copper bicrystals, always nucleated firstly along GBs no matter whether the GBs are perpendicular or parallel to the stress axis. Whereas, for the copper multicrystals containing low-angle GBs, the persistent slip bands (PSBs) are always the preferential sites to initiate fatigue cracks no matter whether low-angle GBs are perpendicular or parallel to the stress axis.

Additionally, the fatigue lives of the GBs, and the $[\bar{1}23]$ and $[\bar{3}35]$ grains in the $[\bar{1}23]\perp[\bar{3}35]$ and $[\bar{5}913]\perp[\bar{5}79]$ bicrystals were measured at different cyclic stresses and strain amplitudes. The results show that intergranular fracture always occurred prior to transgranular fracture in those bicrystals. The fatigue lives increased in the order of the GB, the $[\bar{1}23]$ and the $[\bar{3}35]$ grains in the $[\bar{1}23]\perp[\bar{3}35]$ bicrystal under cyclic tension–tension loading. On the other hand, the fatigue life of the GB in the $[\bar{5}913]\perp[\bar{5}79]$ bicrystal is about two to three times higher than that in the $[\bar{1}23]\perp[\bar{3}35]$ bicrystal. Based on these experimental results from the copper bicrystals and multicrystals, it is indicated that the possibility of fatigue cracking increased in the order of low-angle GBs, PSBs and large-angle GBs. It is suggested that both the PSB–GB mechanism and the step mechanism required for GB fatigue cracking were questionable, and the interaction modes of PSBs with GBs may be more important for intergranular fatigue cracking.

Keywords—Fatigue cracking; Fatigue lives; Large-angle GBs; Low-angle GBs; PSBs.

INTRODUCTION

Fatigue crack initiation and propagation are important processes in the fatigue failure of metallic materials. It has been recognized that the interfaces of PSBs with the matrix are the preferential sites to initiate fatigue cracks in both single crystals [1–6] and polycrystals [7–11]. The fatigue cracking mechanism along PSBs has been proposed and developed by Essmann *et al.* [12], and Repetto and Ortiz [13]. Based on the fatigue cracking along PSBs, the volume fraction of PSBs has been considered as a fatigue damage parameter when predicting the fatigue life of polycrystals [9–11]. On the other hand, in polycrystalline materials, it is found that GBs [14–19] and twin boundaries (TBs) [20–22] can also become the preferential sites leading to fatigue cracking. The crystallographic conditions and dislocation mechanisms of intergranular fatigue cracking have been analysed by Kim and Laird [14,15], Chang [16], and Christ [17]. In fact, GB fatigue cracking is a major mode of fatigue damage in polycrystalline materials, and the failure of polycrystalline materials always occurred at the weakest site. However, it is not clear which is the most preferential site for fatigue cracking. It is definitely necessary to determine the weakest site leading to fatigue cracking among GBs, TBs and PSBs for a better understanding of fatigue damage in polycrystalline materials. In general, bicrystals are widely employed to study the plastic deformation mechanism [23]. However, studies on fatigue cracking along GBs and PSBs in bicrystals are very limited [24–29]. In this paper, we determine the most favourable site for fatigue cracking among large-angle GBs, low-angle GBs and PSBs by using copper bicrystals and copper multicrystals.

EXPERIMENTAL PROCEDURE

Some bicrystal plates of size of $120 \times 50 \times 10\ mm^3$ were grown from OFHC copper of 99.999% purity by the Bridgman method in a horizontal furnace, and the large-angle GB was along the growth direction. Four groups of fatigue specimens were spark-machined from these bicrystal plates, as shown in Fig. 1(a)–(d). The component crystal orientations in those bicrystals were determined by the X-ray Laue back-reflection method and are shown in Fig. 2. The $[\bar{1}23] \perp [\bar{3}35]$ and $[\bar{5}913] \perp [\bar{5}79]$ copper bicrystals had a large-angle GB perpendicular to the stress axis, and the $[\bar{6}79] \parallel [\bar{1}45]$ and $[\bar{3}610] \parallel [\bar{4}57]$ copper bicrystals had a large-angle GB parallel to the stress axis. The fatigue specimens in Fig. 1(a) and (b) are used to compare the fatigue cracking possibility between the large-angle GBs and PSBs in the $[\bar{1}23] \perp [\bar{3}35]$, $[\bar{5}913] \perp [\bar{5}79]$, $[\bar{6}79] \parallel [\bar{1}45]$ and $[\bar{3}610] \parallel [\bar{4}57]$ copper bicrystals under cyclic push–pull straining. The fatigue specimens in Fig. 1(c) and (d) are used to measure the fatigue lives of the GBs, $[\bar{1}23]$ and $[\bar{3}35]$ grains in the $[\bar{1}23] \perp [\bar{3}35]$ copper bicrystal under cyclic tension–tension loading.

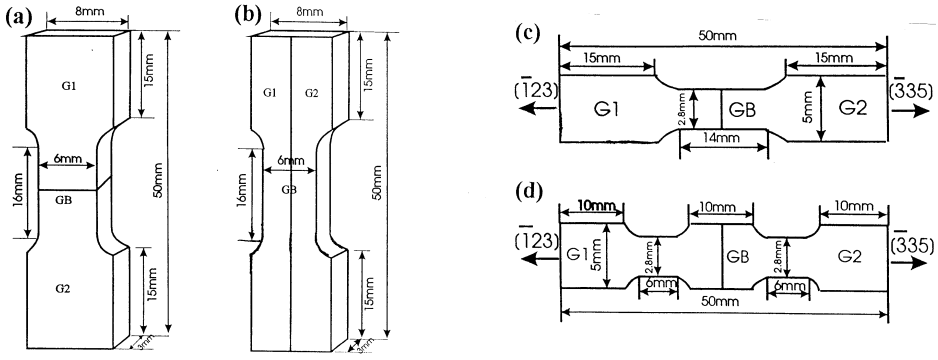

Fig. 1. Fatigue specimens of copper bicrystals. (a) The bicrystal with a horizontal GB. (b) The bicrystal with a vertical GB. (c) The specimen used to measure the GB fatigue life. (d) The specimen used to measure the fatigue life of the $[\bar{1}23]$ and $[\bar{3}35]$ grains.

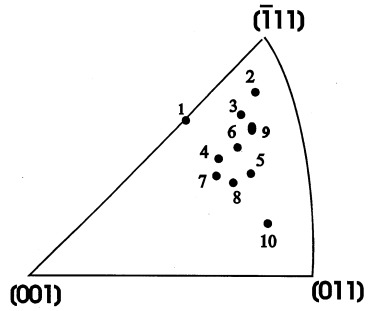

Fig. 2. The orientations of component grains in the bicrystals and multicrystals, where, $1 = [\bar{3}35]$; $2 = [\bar{6}79]$; $3 = [\bar{4}57]$; $4 = [\bar{4}69]$; $5 = [\bar{3}711]$; $6 = [\bar{1}23]$; $7 = [\bar{5}913]$; $8 = [\bar{3}610]$; $9 = [\bar{5}79]$; $10 = [\bar{1}45]$.

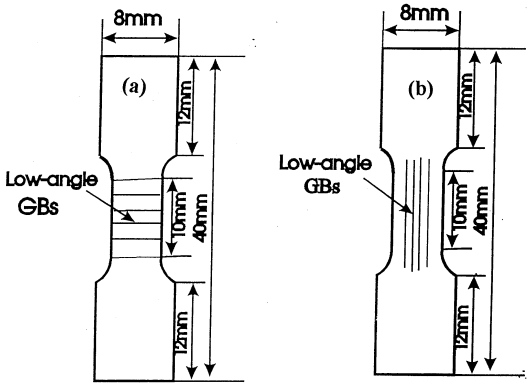

Fig. 3. Fatigue specimens of the $[\bar{3}711]$ and $[\bar{4}69]$ multicrystals. (a) Fatigue specimen of a $[\bar{4}69]$ multicrystal with horizontal low-angle GBs. (b) Fatigue specimen of a $[\bar{3}711]$ multicrystal with vertical low-angle GBs.

Table 1. Control modes during fatigue testing of different crystals

Specimen type	Control mode	Purpose
$[\bar{1}23]\perp[\bar{3}35]$ bicrystal	T–T stress	Fatigue life (N_f)
$[\bar{1}23]\perp[\bar{3}35]$ bicrystal	T–C strain	N_f and cracking
$[\bar{5}913]\perp[\bar{5}79]$ bicrystal	T–C strain	N_f and cracking
$[\bar{6}79]\parallel[\bar{1}45]$ bicrystal	T–C strain	Fatigue cracking
$[\bar{3}610]\parallel[\bar{4}57]$ bicrystal	T–C strain	Fatigue cracking
$[\bar{3}\,7\,11]\parallel$ multicrystal	T–C stress	Fatigue cracking
$[\bar{4}69]\perp$ multicrystal	T–C stress	Fatigue cracking

In addition, two copper multicrystal plates containing some low-angle GBs were also grown from OFHC copper of 99.999% purity. Two kinds of fatigue specimens with low-angle GBs, basically parallel or perpendicular to the stress axis, were prepared from the multicrystal plate, as shown in Fig. 3(a) and (b). The axis orientations of the multicrystal specimens were $[\bar{3}711]$ and $[\bar{4}69]$ on average, respectively, and the misorientation between the adjacent grains was in the range of about 5°. By using the specimens in Fig. 3(a) and (b), the fatigue cracking along low-angle GBs and PSBs can be compared.

Before cyclic deformation, all the fatigue specimens were carefully electro-polished for surface observation. Fatigue tests were performed on a Shimadzu servo-hydraulic testing machine at room temperature in air. The testing methods and purposes are listed in Table 1, where, T–T stress represents tension–tension stress control; T–C strain represents tension–compression strain control.

EXPERIMENTAL RESULTS

Fatigue cracking of copper bicrystals with a perpendicular GB

At a plastic strain range from 2.1×10^{-4} to 2.56×10^{-3}, both $[\bar{1}23]\perp[\bar{3}35]$ and $[\bar{5}913]\perp[\bar{5}79]$ copper bicrystals exhibited a rapid cyclic hardening and saturation behaviour. With further cyclic straining, a rapid cyclic softening corresponding to fatigue crack initiation and propagation can be found. Surface observations by SEM showed that all the fatigue cracks initiated and propagated along the GB in both $[\bar{1}23]\perp[\bar{3}35]$ and $[\bar{5}913]\perp[\bar{5}79]$ bicrystals. The intergranular fatigue cracks of the $[\bar{1}23]\perp[\bar{3}35]$ and $[\bar{5}913]\perp[\bar{5}79]$ bicrystals are shown in Fig. 4(a) and (b). However, fatigue cracking along PSBs was not observed on the surfaces of $[\bar{1}23]\perp[\bar{3}35]$ and $[\bar{5}913]\perp[\bar{5}79]$ bicrystals either at low (2.1×10^{-4}) or high plastic strain amplitude (2.56×10^{-3}). These results are consistent with the observations in the $[\bar{3}45]\perp[\bar{1}17]$ and $[001]\perp[\bar{1}49]$ copper bicrystals by Hu and Wang [27,28], and Peralta and Laird [29]. Since the fatigue failures of those bicrystals were always caused by intergranular cracking, the cycles to failure can be regarded as the GB fatigue lives. The curves of GB fatigue life versus axial plastic strain amplitude in the $[\bar{1}23]\perp[\bar{3}35]$ and $[\bar{5}913]\perp[\bar{5}79]$ bicrystals are shown in Fig. 5(a). It is seen that there is a significant difference in the GB fatigue lives between the two bicrystals. The average GB life of the $[\bar{5}913]\perp[\bar{5}79]$ bicrystal is about two–three times higher than that of the $[\bar{1}23]\perp[\bar{3}35]$ bicrystal.

In addition, the fatigue life of the $[\bar{1}23]\perp[\bar{3}35]$ bicrystal was measured using the fatigue specimen in Fig. 1(c) and (d) under cyclic tension–tension loading. The results showed that all the bicrystals failed by GB cracking. By observing the failed bicrystal surface, the fatigue cracks within the $[\bar{1}23]$, $[\bar{3}35]$ grains are listed in Table 2. It is seen that the fatigue crack on the $[\bar{3}35]$ grain only initiated at higher cyclic loads (950, 1000 and 1125 N), as shown in Fig. 4(c). However, the fatigue crack on the $[\bar{1}23]$ grain can initiate at relatively lower cyclic loads (850, 875, 900, 1000 and 1125 N), as shown in Fig. 4(d). Even though some fatigue cracks on the surfaces of grains can initiate along PSBs, the GB cracking always led to the final failure of the bicrystal.

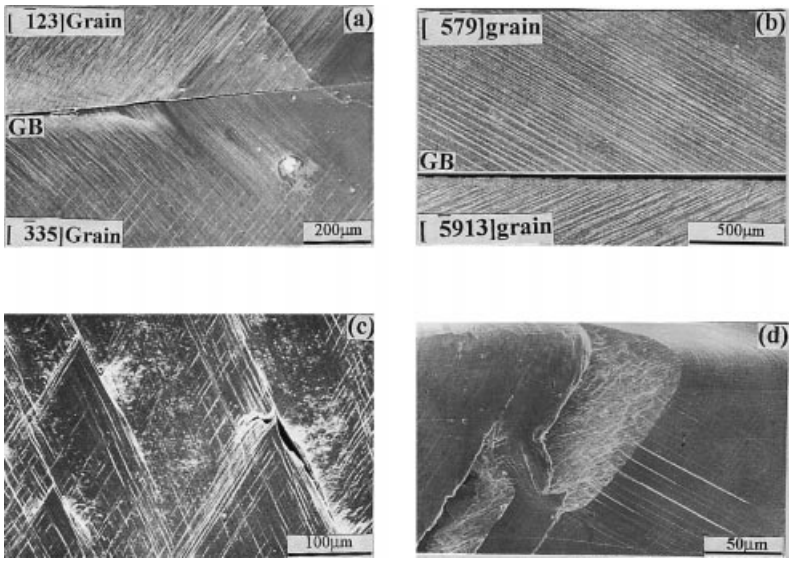

Fig. 4. Fatigue cracks in the copper bicrystals. (a) Intergranular fatigue cracking in the $[\bar{1}23]\perp[\bar{3}35]$ bicrystal ($\varepsilon_{pl} = 6.5 \times 10^{-4}$, $N_f = 7300$ cycles). (b) Intergranular fatigue cracking in the $[\bar{5}913]\perp[\bar{5}79]$ bicrystal ($\varepsilon_{pl} = 1.35 \times 10^{-3}$, $N_f = 6700$ cycles). (c) Fatigue cracks along slip bands within the $[\bar{3}35]$ grain ($P = 1000$ N, $N_f = 1\,150\,000$ cycles). (d) Fatigue cracks along slip bands within the $[\bar{1}23]$ grain ($P = 900$ N, $N_f = 1\,910\,000$ cycles).

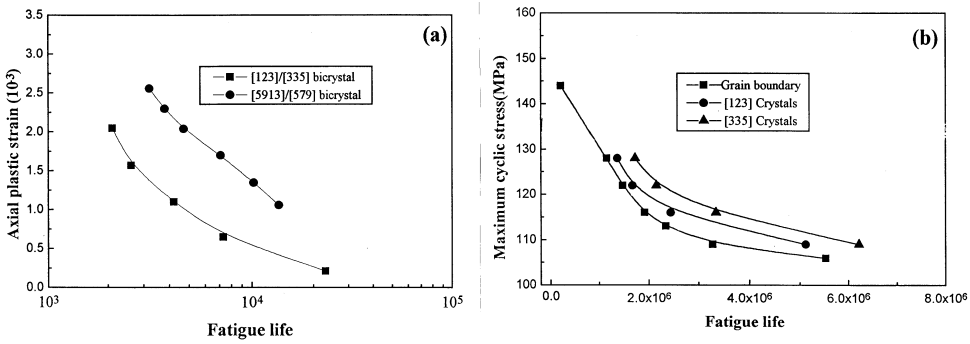

Fig. 5. Fatigue life curves for the $[\bar{1}23]\perp[\bar{3}35]$ and $[\bar{5}913]\perp[\bar{5}79]$ bicrystals. (a) GB fatigue life curves in the $[\bar{1}23]\perp[\bar{3}35]$ and $[\bar{5}913]\perp[\bar{5}79]$ bicrystals. (b) Fatigue life curves of the GB, $[\bar{1}23]$ and $[\bar{3}35]$ grains in the $[\bar{1}23]\perp[\bar{3}35]$ bicrystal.

Figure 5(b) shows the curves of the fatigue life versus nominal maximum cyclic stress of the GB, $[\bar{1}23]$ and $[\bar{3}35]$ grains in the $[\bar{1}23]\perp[\bar{3}35]$ bicrystal under cyclic tension–tension loading. The nominal maximum cyclic stress is defined as the maximum cyclic tension load divided by the original area (2.8×2.8 mm^2) of the specimen. It is found that the fatigue life increases in the order of GB, $[\bar{1}23]$ and $[\bar{3}35]$ grain under the same cyclic tension–tension load.

Fatigue cracking of copper bicrystals with a parallel GB

Cyclic deformation studies were performed on both $[\bar{6}79]\parallel[\bar{1}45]$ and $[\bar{3}610]\parallel[\bar{4}57]$ bicrystals with a parallel GB under a total strain amplitude of 2×10^{-3}. The tests were interrupted at certain

Table 2. The possibility of fatigue cracking in component crystals

[$\bar{1}$23] crystal	[$\bar{3}$35] crystal	GB life (cycles)	Maximum load (N)	Minimum load (N)
+	+	209 000	1125	125
+	+	1 150 000	1000	125
+	+	1 470 000	950	125
+	−	1 910 000	900	125
+	−	2 340 000	875	125
+	−	3 280 000	850	125
−	−	5 530 000	825	125
−	−	12 000 000	800	125

+ Cracking; − No cracking.

cycles for observing, by SEM, the initiating fatigue crack. The results show that the strain incompatibility in the vicinity of the GB became more serious with increasing cyclic number. When the number of cycles was over 10^4, fatigue cracking in both the [$\bar{6}$79] ∥ [$\bar{1}$45] and [$\bar{3}$610] ∥ [$\bar{4}$57] bicrystals can be observed, as shown in Fig. 6(a) and (b), and all fatigue cracks are of the intergranular type. However, no apparent fatigue cracking along PSBs was found on the component grain surface, excepting some extrusions [see Fig. 6(c)]. These results indicated that the GBs in those bicrystals are also the preferential sites leading to fatigue cracking even though they are parallel to the stress axis.

Fatigue cracking of copper multicrystals containing low-angle GBs

In order to compare the possibility of fatigue cracking along low-angle GBs and PSBs, the specimens containing some low-angle GBs [Fig. 3(a) and (b)] were first subjected to cyclic push–

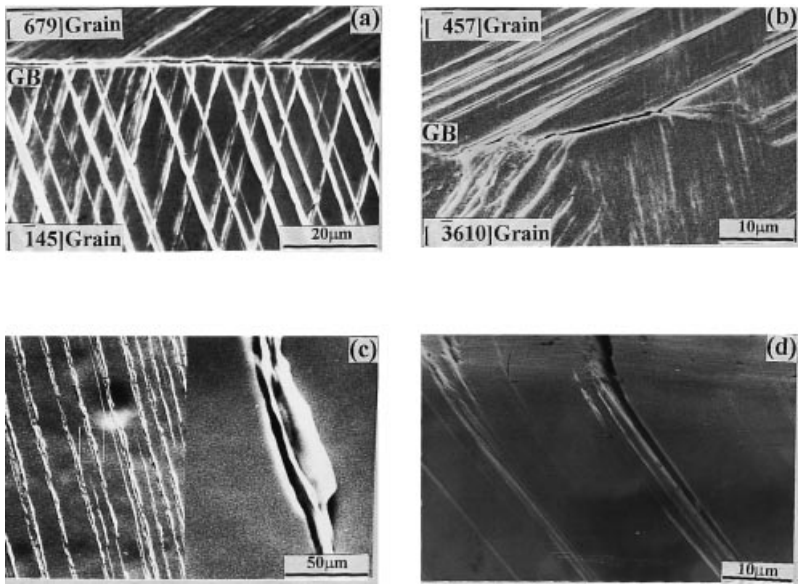

Fig. 6. Fatigue cracks in the [$\bar{6}$79] ∥ [$\bar{1}$45] and [$\bar{3}$610] ∥ [$\bar{4}$57] bicrystals. (a) Intergranular crack in the [$\bar{6}$79] ∥ [$\bar{1}$45] bicrystal ($\varepsilon_a = 2 \times 10^{-3}$, $N = 3 \times 10^4$). (b) Intergranular crack in the [$\bar{3}$610] ∥ [$\bar{4}$57] bicrystal ($\varepsilon_a = 2 \times 10^{-3}$, $N = 5 \times 10^4$). (c) The PSBs of [$\bar{6}$79] grain in the [$\bar{6}$79] ∥ [$\bar{1}$45] bicrystal ($\varepsilon_a = 2 \times 10^{-3}$, $N = 3 \times 10^4$). (d) Fatigue cracking along PSBs in the [$\bar{4}$69] multicrystal ($\sigma_a = 62$ MPa, $N = 12 \times 10^4$ cycles).

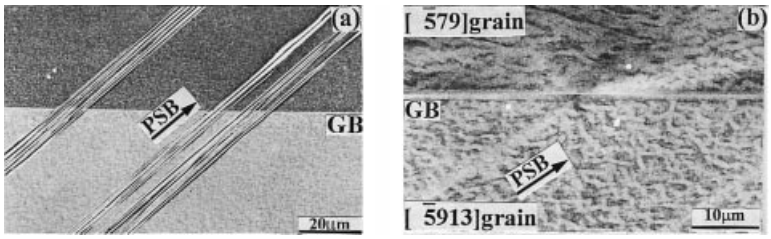

Fig. 7. The interactions of PSBs with GBs. (a) PSBs passing through a low-angle GB as observed by the ECC technique. (b) The interaction of PSB with a large-angle GB in the $[\bar{5}913]\perp[\bar{5}79]$ bicrystal as observed by the ECC technique.

pull deformation by step loading from 10 to 62 MPa ($[\bar{3}711]$) and 68 MPa ($[\bar{4}69]$), respectively. Then, the constant stress amplitudes of 62 and 68 MPa were performed on the two multicrystals continuously until a fatigue crack initiated. These stresses correspond to the resolved shear stresses activating the PSBs within the $[\bar{3}711]$ and $[\bar{4}69]$ multicrystals. The results showed that the number of cycles for fatigue cracking was obviously higher than that in bicrystals, and all the fatigue cracks nucleated along PSBs, as shown in Fig. 5(d). No fatigue cracks were found along the existing low-angle GBs. To reveal the interactions of low-angle GBs with PSBs, the electron channelling contrast (ECC) technique was employed, as reported in Refs [30–32]. The ECC technique proved that the PSBs can pass through the low-angle GBs continuously [see Fig. 7(a)] rather than terminate at the GBs. In contrast, the PSBs can not pass through the large-angle GB in copper bicrystals, as shown in Fig. 7(b). These results indicate that the strain should be compatible in the vicinity of the low-angle GBs, but not in the large-angle GBs.

DISCUSSION

Comparison of fatigue cracking between large-angle GBs and PSBs

It has been well determined that the preferential sites for fatigue cracking in pure metals are PSBs and GBs. A model of fatigue cracking along PSBs was proposed and developed by Essmann *et al.* [12], and Repetto and Ortiz [13] in single crystals. Meanwhile, a PSB–GB interaction mechanism was developed and has been successfully used to explain the possibility of intergranular fatigue cracking at intermediate plastic strains [14–18]. In high strain fatigue, GB steps develop on the specimen surface. The step size increases with increasing number of cycles and fatigue cracks nucleated near these steps [15]. It is indicated that both PSBs and GBs will become the possible sites to nucleate fatigue cracks in polycrystalline materials. However, the results which favour fatigue cracking between PSBs and GBs are different and even controversial. Vehoff *et al.* [25] have examined the influence of orientation, segregation and hydrogen on fatigue crack initiation in nickel bicrystals. They found that the PSB cracking within the component grains occurred in preference to intergranular cracking if the GBs are clean. For nickel polycrystals, it is found that in air, surface intergranular cracking occurred early in fatigue life and is induced by the impinging slip traces at the interface at 573 K [19]. For α–β brass two-phase bicrystals with a GB parallel to the stress axis, Kawazoe *et al.* [26] found that the fatigue crack always initiated at the edge of the α phase near the shoulder section rather than at the multiple slip region near the interface. This behaviour differs from the results of mono-phase bicrystals where the cracks nucleated in the boundary affected zone [24].

From these results on fatigue cracking behaviour in copper bicrystals and from Refs [27–29],

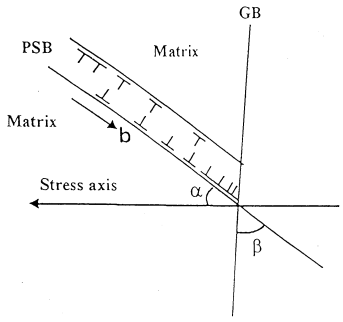

Fig. 8. The geometrical relations among the PSB, GB and stress axis required for the PSB–GB mechanism.

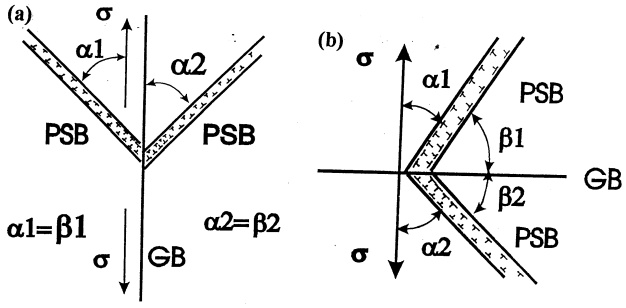

Fig. 9. The geometrical relations among the PSB, GB and stress axis in the copper bicrystals. (a) The copper bicrystals with the GB perpendicular to the stress axis. (b) The copper bicrystals with the GB parallel to the stress axis.

it can be concluded that the large-angle GBs will be the preferential sites leading to fatigue cracking in comparison with PSBs. Some geometrical conditions required for the PSB–GB mechanism of intergranular cracking are shown in Figure 8. The favourable angles of α and β suggested by Christ [17] are 45° and 70.5°, respectively, for intergranular cracking. The geometrical relations between GB, PSBs and the stress axis are shown in Fig. 9(a) and (b) for the $[\bar{1}23]\perp[\bar{3}35]$, $[\bar{5}913]\perp[\bar{5}79]$, $[\bar{6}79]\parallel[\bar{1}45]$ and $[\bar{3}610]\parallel[\bar{4}57]$ bicrystals. The values of angles α and β are calculated and listed in Table 3 according to the crystallographic relation in those bicrystals. It can be found that the geometrical conditions in those bicrystals are not completely consistent with those required for the PSB–GB intergranular cracking mechanism. From the geometrical conditions between PSBs, GB and stress axis (see Table 3) in these bicrystals, it seems that the PSB–GB mechanism is unsuitable for the present results. In particular, the step-mechanism proposed by Kim and Laird [14,15] can not successfully explain why intergranular fatigue cracking always occurred in the $[\bar{6}79]\parallel[\bar{1}45]$ and $[\bar{3}610]\parallel[\bar{4}57]$ bicrystals with a perpendicular GB.

Comparison of fatigue cracking between low-angle GBs and PSBs

It was reported [24] that low-angle GBs permitted slip bands to cross through and cracks formed in the boundary; whereas large-angle GBs caused slip bands to be terminated and crack initiated in slip bands. The authors suggested that compatible deformation will promote crack nucleation in the GBs and incompatible deformation will lead to slip band cracking. In contrast,

Table 3. The interaction angles among the PSB, GB and stress axis in bicrystals and multicrystals

	α_1 (°)	β_1 (°)	α_2 (°)	β_2 (°)
$[\bar{1}23]\perp[\bar{3}35]$	40.9	49.1	30.4	59.6
$[\bar{5}913]\perp[\bar{5}79]$	39.9	50.1	37.3	52.7
$[\bar{6}79]\parallel[\bar{1}45]$	34.6	34.6	49.1	49.1
$[\bar{3}610]\parallel[\bar{4}57]$	40.2	40.2	34.9	34.9
$[\bar{3}711]\parallel$	42.3	42.3	42.3	42.3
$[\bar{4}69]\perp$	37.1	52.9	37.1	52.9

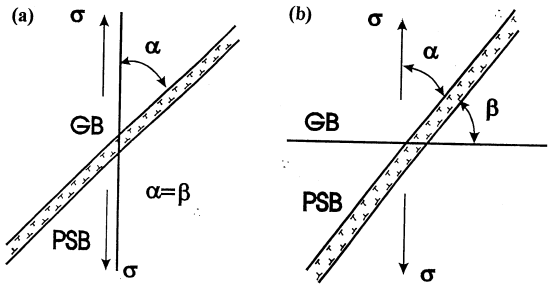

Fig. 10. The geometrical relations among the PSB, GB and stress axis in the copper multicrystals. (a) The copper multicrystals with the GB perpendicular to the stress axis. (b) The copper multicrystals with the GB parallel to the stress axis.

the present observations on multicrystals indicate that fatigue crack always initiated along PSBs rather than along low-angle GBs [see Fig. 5(d)] even though these GBs are all of the low-angle type.

The geometrical relations between GB, PSBs and the stress axis in the two kinds of multicrystals are shown in Fig. 10(a) and (b). The interaction angles of α and β were also calculated according to their crystallographic relations and are listed in Table 3. It can be seen that the geometrical conditions are also not consistent with those required for the PSB–GB mechanism and the fatigue cracking was not along the low-angle GBs. These experimental results clearly indicate that the fatigue cracking possibility among large-angle GBs, low-angle GBs and PSBs is quite different, even though the geometrical relations among GBs, PSBs and the stress axis are basically similar. This implies that the PSB–GB mechanism for intergranular cracking is also questionable. This leads to two questions: what dominates intergranular cracking; and what is the exact mechanism for it?

Essentially, the geometrical relations between PSB, GB and the stress axis can be considered as a criteria leading to intergranular fatigue cracking, from which it can be determined whether intergranular cracking is easy or difficult for a given GB. The results quoted indicate that fatigue cracking always occurred along the large-angle GBs in bicrystals, but preferred the PSBs in multicrystals, even though the geometrical conditions required for PSB–GB mechanisms between large-angle GBs and low-angle GBs are basically similar. Thus, intergranular fatigue cracking may be an intrinsic phenomenon for the large-angle GBs and the interaction-modes of PSBs with different kinds of GBs might be more important.

By the ECC technique, the interactions of PSBs with large-angle GBs and low-angle GBs have been revealed. Fig. 8(b) illustrates the interaction of a PSB with a large-angle GB in bicrystals. It can be seen that the large-angle GB will become a barrier against PSBs passing through. However, the PSBs across a low-angle GB are basically coplanar, as shown in Fig. 8(a). This implies that low-angle GBs permit PSBs to pass through. It is well known that most plastic strains are carried by PSBs during cyclic deformation in metallic materials. The PSB may become a carrier and a channel transporting residual dislocations and vacancies from the interior of grains into the GBs. As the residual dislocations and vacancies were piled-up at a large-angle GB and accumulated to become high enough in density, the intergranular cracking along the GB will occur under external cyclic stress. However, the PSBs beside a low-angle GB are nearly coplanar owing to lower misorientations. In this case, the residual dislocations and vacancies may not build up at the low-angle GBs, but be moved into the adjacent grain. This may explain why a fatigue crack does not initiate along the low-angle GBs and the interface of PSBs with the matrix will become the preferential sites for fatigue cracking, as shown in Fig. 5(d).

Comparison of fatigue lives among different kinds of GBs

It can be seen [from Fig. 5(a)] that the GB fatigue life in the $[\bar{5}913]\perp[\bar{5}79]$ bicrystal is about two–three times higher than that in the $[\bar{1}23]\perp[\bar{3}35]$ bicrystal. It has been recognized that the plastic strains carried by two grains in a bicrystal with a perpendicular GB are different owing to the difference in crystal orientations [29]. The soft grain with a relatively higher Schmid factor will carry more plastic strain than the hard one. For the $[\bar{1}23]\perp[\bar{3}35]$ and $[\bar{5}913]\perp[\bar{5}79]$ bicrystals, the Schmid factors of their component grains are $\Omega_{[\bar{1}23]}=0.467$, $\Omega_{[\bar{3}35]}=0.380$, $\Omega_{[\bar{5}913]}=0.452$ and $\Omega_{[\bar{5}79]}=0.406$, respectively. I.e. the Schmid factors of these component grains increase in the following order,

$$\Omega_{[\bar{3}35]}<\Omega_{[\bar{5}79]}<\Omega_{[\bar{5}913]}<\Omega_{[\bar{1}23]}$$

When the same plastic strain is applied to the $[\bar{1}23]\perp[\bar{3}35]$ and $[\bar{5}913]\perp[\bar{5}79]$ bicrystals, the

plastic strains carried by these component grains will decrease in the following order,

$$\varepsilon_{[\bar{1}23]} > \varepsilon_{[\bar{5}913]} > \varepsilon_{[\bar{5}79]} > \varepsilon_{[\bar{3}35]}$$

Thus, we have

$$\varepsilon_{[\bar{1}23]} - \varepsilon_{[\bar{3}35]} > \varepsilon_{[\bar{5}913]} - \varepsilon_{[\bar{5}79]}$$

As a result, there will be a difference in plastic strain across the GB plane in those bicrystals. With an increasing difference in the Schmid factor between the two component grains, the degree of plastic strain inhomogeneity at a GB will also become more serious. By analysing the plastic strain distribution at the GB in two bicrystals, it is clear that the inhomogeneity of plastic strain by the GB in the $[\bar{1}23]\perp[\bar{3}35]$ bicrystal is higher than that in the $[\bar{5}913]\perp[\bar{5}79]$ bicrystal. This may be the reason why the $[\bar{5}913]\perp[\bar{5}79]$ bicrystal shows a relatively higher fatigue life than the $[\bar{1}23]\perp[\bar{3}35]$ bicrystal.

CONCLUSIONS

Based on our experimental results, the following conclusions can be drawn.

(1) The fatigue cracks always initiated firstly at the large-angle GBs in copper bicrystals, no matter whether the GBs are perpendicular or parallel to the stress axis.
(2) The GB fatigue life is always short when compared to those of the $[\bar{1}23]$ and $[\bar{3}35]$ grains in the $[\bar{1}23]\perp[\bar{3}35]$ copper bicrystal under cyclic tension–tension loading. Furthermore, the GB fatigue lives of the $[\bar{1}23]\perp[\bar{3}35]$ and $[\bar{5}913]\perp[\bar{5}79]$ copper bicrystals showed a significant difference, which may be attributed to the difference in orientations.
(3) PSBs are favourable sites for fatigue cracking in copper multicrystals as compared to low-angle GBs.
(4) The possibility of fatigue cracking increased in the order of low-angle GBs, PSBs and large-angle GBs.
(5) It is suggested that both the step mechanism and PSB–GB mechanism for intergranular cracking are questionable and the interaction modes of PSB with different kinds of GBs may be more important.

Acknowledgements—This work was financially supported by the National Nature Science Foundation of China (NSFC) under grant Nos 19392300-4 and 59701006. The authors are grateful for this support.

REFERENCES

1. Z. S. Basinski and S. J. Basinski (1985) Formation and growth of subcritical fatigue cracks. *Scripta Metall.* **19,** 851–856.
2. Z. S. Basinski and S. J. Basinski (1985) Low amplitude fatigue of copper single crystals, II Surface observation. *Acta Metall.* **33,** 1307–1317.
3. Z. S. Basinski and S. J. Basinski (1985) Low amplitude fatigue of copper single crystals III PSB sections. *Acta Metall.* **33,** 1319–1327.
4. A. Hunsche and P. Neumann (1986) Quantitative measurement of persistent slip band profiles and crack initiation. *Acta Metall.* **34,** 207–217.
5. P. Neumann (1992) The effect of surface related grain boundary stress of fatigue. *Scripta Metall. Mater.* **26,** 1535–1540.
6. H. Mughrabi (1992) Introduction to the viewpoint set on: Surface effects in cyclic deformation and fatigue. *Scripta Metall. Mater.* **26,** 1499–1504.
7. F.-L. Liang and C. Laird (1989) Control of intergranular fatigue cracking by slip homogeneity in copper, I. Effect of grain size. *Mater. Sci. Engng* **A117,** 103–113.

8. F.-L. Liang and C. Laird (1989) Control of intergranular fatigue cracking by slip homogeneity in copper, II. Effect of loading modes. *Mater. Sci. Engng* **A117,** 114–123.
9. L. A. Ahmadieh and P. K. Mazumdar (1988) A cumulative fatigue damage formulation for persistent slip band type materials. *Scripta Metall.* **22,** 1761–1764.
10. W. D. Cao and H. Conrad (1992) On the effect of persistent slip band parameters on fatigue life. *Fatigue Fract. Engng Mater. Struct.* **15,** 573–583.
11. J. Polak, A. Vasek and K. Obrtlik (1996) Fatigue damage in two step loading of 316L steel, I Evolution of persistent slip bands. *Fatigue Fract. Engng Mater. Struct.* **19,** 147–155.
12. U. Essmann, U. Gosele and H. Mughrabi (1981) A model of extrusions and intrusions in fatigued metals, I: Point-defect production and the growth of extrusions. *Phil. Mag.* **A44,** 405–426.
13. E. A. Repetto and M. Ortiz (1997) A micromechnical model of cyclic deformation and fatigue crack nucleation in f.c.c. single crystals. *Acta Mater.* **45,** 2577–2595.
14. W. H. Kim and C. Laird (1978) Crack nucleation and stage I propagation in high strain fatigue, I. Microscopic and interferometric observation. *Acta Metall.* **26,** 777–787.
15. W. H. Kim and C. Laird (1978) Crack nucleation and stage I propagation in high strain fatigue, II. Mechanism. *Acta Metall.* **26,** 789–799.
16. R. Chang (1979) A dislocation mechanism of grain boundary crack nucleation and growth under low cyclic stresses. *Scripta Metall.* **13,** 1079–1081.
17. H.-J. Christ (1989) On the orientation of cyclic-slip-induced intergranular fatigue cracks in face-centered cubic metals. *Mater. Sci. Engng* **A117,** L25–L29.
18. W. Liu, M. Bayerlein, H. Mughrabi, A. Day and P. N. Quested (1992) Crystallographic feature of intergranular crack initiation in fatigued copper polycrystals. *Acta. Metall. Mater.* **40,** 1763–1771.
19. L. C. Lim (1987) Surface intergranular cracking in large strain fatigue. *Acta. Metall.* **35,** 1653–1662.
20. R. C. Boettner, A. J. McEvily and Y. C. Liu (1964) On the formation of fatigue crack at twin boundaries. *Phil. Mag.* **9,** 95–106.
21. A. Heinz and P. Neumann (1990) Crack initiation during high cyclic fatigue of an austenitic steel. *Acta Metall. Mater.* **38,** 1933–1940.
22. X. L. Tan and H. C. Gu (1994) The effect of grain boundaries on fatigue behavior in high purity titanium. In: *Strength of Materials* (Edited by H. Oikawa, K. Maruyama, S. Takeuchi and M. Yamaguchi), The Japan Institute of Metals, pp. 163–166.
23. J. P. Hirth (1972) The influence of grain boundaries on mechanical properties. *Metall. Trans.* **3,** 3047–3067.
24. J. C. Swearengen and R. Targgart (1971) Low amplitude cyclic deformation and crack nucleation in copper and copper-aluminum bicrystals. *Acta Metall.* **19,** 543–559.
25. H. Vehoff, C. Laird and D. J. Duquette (1987) The effects of hydrogen and segregation on fatigue crack nucleation at defined grain boundaries in nickel bicrystals. *Acta Metall.* **35,** 2877–2886.
26. H. Kawazoe, T. Takasugi and O. Izumi (1989) Cyclic deformation of α–β brass two-phase bicrystals, I. Slip behavior. *Acta Metall.* **37,** 2883–2894.
27. Y. M. Hu and Z. G. Wang (1996) Fatigue crack initiation and early growth in a copper bicrystal with a grain boundary perpendicular to stress axis. *Scripta Mater.* **35,** 1019–1025.
28. Y. M. Hu and Z. G. Wang (1997) Low cycle fatigue of a copper bicrystal under constant plastic strain control. *Int. J. Fatigue* **19,** 59–65.
29. P. Peralta and C. Laird (1997) The role of strain compatibility in the cyclic deformation of copper bicrystals. *Acta Mater.* **45,** 3029–3046.
30. R. Zauter, F. Petry, M. Bayerlein, C. Sommer, H. Christ and H. Mughrabi (1992) Electron channelling contrast as a supplementary method for microstructural investigation in deformed metals. *Phil. Mag.* **A66,** 425–436.
31. A. Schwab, J. Bretschneider, C. Buque, C. Blochwitz and C. Holste (1996) Application of electron channelling contrast to the investigation of strain localization effects in cyclically deformed fcc metals. *Phil. Mag. Lett.* **74,** 449–454.
32. J. Bretschneider, C. Holste and B. Tippelt (1997) Cyclic plasticity of nickel single crystals at elevated temperature. *Acta Mater.* **45,** 3775–3783.

